World Journal of Radiology

Online Submissions: http://www.wjgnet.com/esps/
bpgoffice@wjgnet.com
doi:10.4329/wjr.v5.i11.421

World J Radiol 2013 November 28; 5(11): 421-429
ISSN 1949-8470 (online)

ORIGINAL ARTICLE

CT dose and image quality in the last three scanner generations

Andreas Christe, Johannes Heverhagen, Christoph Ozdoba, Christian Weisstanner, Stefan Ulzheimer, Lukas Ebner

Andreas Christe, Johannes Heverhagen, Lukas Ebner, Department of Radiology, University Hospital of Bern, Inselspital, 3010 Bern, Switzerland
Christoph Ozdoba, Christian Weisstanner, Department of Neuroradiology, University Hospital of Bern, Inselspital, 3010 Bern, Switzerland
Stefan Ulzheimer, Siemens AG Healthcare, An der Lände 1, 91301 Forchheim, Germany
Author contributions: Ebner L, Christe A performed the majority of the experiments; Ozdoba C, Weisstanner C coordinated the experiments with the Somatom Definition Edge Scanner and were also involved in editing the manuscript; Ulzheimer S, Heverhagen J performed the physical, mathematical and technical review and edited the manuscript; Christe A, Ebner L designed the study and wrote the manuscript.
Correspondence to: Andreas Christe, MD, Departement of Radiology, University Hospital of Bern, Inselspital, Freiburgstrasse 10, 3010 Bern, Switzerland. andreas.christe@insel.ch
Telephone: +41-31-6321965 Fax: +41-31-6324874
Received: July 17, 2013 Revised: September 24, 2013
Accepted: November 2, 2013
Published online: November 28, 2013

Abstract

AIM: To compare the computed tomography (CT) dose and image quality with the filtered back projection against the iterative reconstruction and CT with a minimal electronic noise detector.

METHODS: A lung phantom (Chest Phantom N1 by Kyoto Kagaku) was scanned with 3 different CT scanners: the Somatom Sensation, the Definition Flash and the Definition Edge (all from Siemens, Erlangen, Germany). The scan parameters were identical to the Siemens presetting for THORAX ROUTINE (scan length 35 cm and FOV 33 cm). Nine different exposition levels were examined (reference mAs/peek voltage): 100/120, 100/100, 100/80, 50/120, 50/100, 50/80, 25/120, 25/100 and 25 mAs/80 kVp. Images from the SOMATOM Sensation were reconstructed using classic filtered back projection. Iterative reconstruction (SAFIRE, level 3) was performed for the two other scanners. A Stellar detector was used with the Somatom Definition Edge. The CT doses were represented by the dose length products (DLPs) (mGycm) provided by the scanners. Signal, contrast, noise and subjective image quality were recorded by two different radiologists with 10 and 3 years of experience in chest CT radiology. To determine the average dose reduction between two scanners, the integral of the dose difference was calculated from the lowest to the highest noise level.

RESULTS: When using iterative reconstruction (IR) instead of filtered back projection (FBP), the average dose reduction was 30%, 52% and 80% for bone, soft tissue and air, respectively, for the same image quality ($P < 0.0001$). The recently introduced Stellar detector (Sd) lowered the radiation dose by an additional 27%, 54% and 70% for bone, soft tissue and air, respectively ($P < 0.0001$). The benefit of dose reduction was larger at lower dose levels. With the same radiation dose, an average of 34% (22%-37%) and 25% (13%-46%) more contrast to noise was achieved by changing from FBP to IR and from IR to Sd, respectively. For the same contrast to noise level, an average of 59% (46%-71%) and 51% (38%-68%) dose reduction was produced for IR and Sd, respectively. For the same subjective image quality, the dose could be reduced by 25% (2%-42%) and 44% (33%-54%) using IR and Sd, respectively.

CONCLUSION: This study showed an average dose reduction between 27% and 70% for the new Stellar detector, which is equivalent to using IR instead of FBP.

Key words: Low dose computed tomography; Comput-

ed tomography image quality; Dose reduction; Computed tomography detector; Image noise; Computed tomography signal to noise

Core tip: A computed tomography dose reduction between 30% and 80% can be expected when using iterative reconstruction instead of filtered back projection. The benefit of dose reduction is larger at lower dose levels. An additional dose reduction between 27% and 70% can be obtained by applying the new Stellar detector.

Christe A, Heverhagen J, Ozdoba C, Weisstanner C, Ulzheimer S, Ebner L. CT dose and image quality in the last three scanner generations. *World J Radiol* 2013; 5(11): 421-429 Available from: URL: http://www.wjgnet.com/1949-8470/full/v5/i11/421.htm DOI: http://dx.doi.org/10.4329/wjr.v5.i11.421

INTRODUCTION

Engineering progress has greatly reduced the radiation dose required for computer tomography. Dose modulation along the x-, y- and z-axes[1-6] and shielding[7-12] represent major manufacturing steps involved in radiation protection. Increasing computing capacity has allowed iterative reconstruction to be introduced in the clinical routine, leading to dose reductions between 27% and 65%[13-18]. Problems with electronic noise during image acquisition can be overcome by integrating analog-digital-converters with the photodiodes on the CT-detectors contained on the same silicon chip (Stellar detector, Siemens Healthcare, Erlangen, Germany) with the potential to further reduce radiation dose[19].

Image quality can be characterized by calculating the noise, signal to noise ratio (SNR) and contrast to noise ratio (CNR)[20-24]. The signal at a region of interest (ROI) corresponds to the attenuation in Hounsfield units (HU). The noise corresponds to the standard deviation of the pixel attenuation within the ROI[20]. The signal will remain the same with lower tube current and unchanged tube voltage, but the noise will increase[21]. Several studies have demonstrated the feasibility of low dose imaging using a lowest acceptable tube current below 50 mAs for lung nodule detection[25-28].

Changing tube voltage changes the signal and the noise, depending on the absorption spectrum of the scanned object[21]. The dose (D) is coupled with many variables: D~(signal to noise)^2/(pixel-size*image-thickness), D~mAs (Miliamperesecond) and D~kVp^2 (Kilovolt peak)[20,21,25]. Noise reduction can either be used for dose reduction or to increase the image quality.

It is not known if the same CT dose is required to generate the same CNR with the new generation of CT scanners. Therefore, we investigated how the lowest acceptable signal to noise acquired at 50 mAs/80 kVp and used for filtered back projection can be transferred to iteratively reconstructed images using a new detector. We compared the dependency of dose and noise (SNR and CNR) for the last three generations of CT scanners.

MATERIALS AND METHODS

Lung phantom

A lung phantom (Chest Phantom N1 by Kyoto Kagaku) was used in this study (Figure 1). This phantom is an accurate life-size anatomical model of a male human torso with a synthetic heart, trachea, pulmonary vessels (right and left) and abdomen (diaphragm) block. The thickness of the chest wall is based on measurement of clinical data. The soft tissue substitute material (polyurethane, gravity 1.06) and synthetic bones (epoxy resin) have X-ray absorption rates very close to those of human tissues. The abducted arm positions of the torso are appropriate for CT scanning. The pulmonary vessels are also spatially traceable.

The phantom size was 43 cm × 40 cm × 48 cm with a chest girth of 94 cm and a weight of 18 kg. The pleural cavity measured 268 mm (craniocaudal). The phantom was measured at the level of the lung apices using axial slices (140 mm × 400 mm) and at the level of the diaphragm (208 mm × 279 mm).

Image acquisition

The phantom was scanned using 3 different CT scanners (Siemens SOMATOM Sensation, SOMATOM Definition Flash and SOMATOM Definition Edge, all from Siemens Healthcare, Erlangen, Germany). The scan parameters were identical to the manufacturer's standard presetting for THORAX ROUTINE: 24 mm × 1.2 mm, pitch 0.8 mm and slice thickness 1.5 mm for the SOMATOM Sensation 64; 128 mm × 0.6 mm, pitch 0.6 and slice thickness 1 mm for the SOMATOM Definition Flash; and 128 mm × 0.6 mm, pitch 0.6 and slice thickness 1 mm for the SOMATOM Definition Edge. The scan length and field of view (FOV) were 35 cm and 33 cm, respectively. Nine different exposition levels were used (reference mAs/tube voltage): 100/120, 100/100, 100/80, 50/120, 50/100, 50/80, 25/120, 25/100 and 25 mAs/80 kV. The option CARE kV setting that automatically adjusts tube voltage to an optimal level was disabled so that we could set the voltage to the predefined values. Reference mAs were used to keep the study parameters as close as possible to those used for routine scans. Images from the SOMATOM Sensation 64 were reconstructed using the classic filtered back projection method with a soft tissue kernel of B20 and a lung kernel of B60. Iterative reconstruction (SAFIRE, level 3) was performed for the two other scanners using the I26f and I70f Kernels. The dose was represented by the dose length product DLP (mGycm) provided by the scanners for a 32 cm diameter phantom for each scan with a constant scan length of 35 cm.

Image analysis

Signal and noise were recorded by two different radiolo-

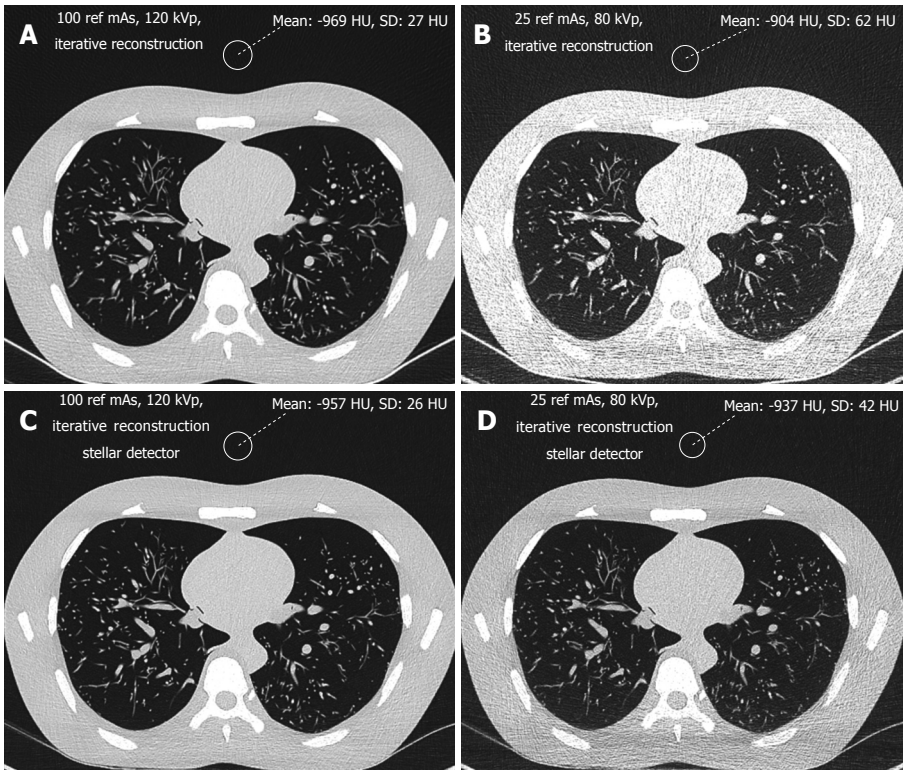

Figure 1 Imaging of the lung using iterative reconstruction with (C, D) and without (A, B) the Stellar detector. The chest phantom was scanned at a standard dose level with a 100 reference mAs tube current time and a 120 kVp voltage (A, C) and the lowest dose level of 25 ref mAs and 80 kVp. At the standard dose level both images with and without the Stellar detector (A,C) had similar noise levels (20-30 HU), while at the lowest dose, the image quality was obviously better with the Stellar detector (D).

gists with 10 and 3 years of experience, respectively, in chest CT radiology using a Picture Archiving and Communication System (PACS Philips Netherlands/Sectra Sweden). They measured the density in HU (signal) and the standard deviation of the CT values (noise) from regions of interest (ROIs) of 2 cm (3.14 cm^2) in diameter. The ROIs were placed in air outside the phantom, anterior to the sternum (Figure 1) in bone (middle of the vertebral body) and soft tissue (heart, Figure 2). Each radiologist chose 5 different levels at which to place the ROIs in the phantom scans. Signal and noise were measured from the same ROIs. Measurements were recorded for air and bone using a hard Kernel and for soft tissue using a soft Kernel. The image quality (SNR) was calculated for soft tissue. Only the noise was recorded for air because the signal in air was negligible. Dose was represented by the dose length product DLP (mGycm) calculated automatically by the scanner for a 32 cm diameter phantom for each scan with a constant scan length of 35 cm. CNR was defined as the difference between the signal from the bone and the soft tissue divided by the noise: HUbone-HUsoft tissue/noise[29].

In addition, both radiologists scored the subjective image quality from 1 to 5 in the lung window (level -500 HU, width 1500 HU, Figure 1) using a hard Kernel on a Picture Archiving and Communication System (PACS Philips Netherlands/Sectra Sweden). The subjective image quality scale was as follows: (1) non-diagnostic; (2) poor, diagnostic confidence significantly reduced; (3) moderate, but sufficient for diagnosis; (4) good; and (5) excellent. Curves were fitted for the noise *vs* dose and for the SNR *vs* dose. The highest R-square correlation coefficients were observed for power curves. For the same noise or same SNR, this allows the corresponding CT acquisition dose for the different scanners to be exactly determined. The lowest acceptable doses of 50 mAs and 80 kVp determined from the filtered back projection method were transferred to image acquisition with iterative reconstruction with Stellar detectors.

Correction factor

To compare the different scans, it was necessary to transform the noise and the dose to obtain the same acquisition parameters as the SOMATOM Sensation. The dose and noise were therefore calculated for a standard slice thickness of 1.5 mm (SOMATOM Sensation). Because the dose remains constant when slice thickness is increased from 1 to 1.5 mm for the new generation Siemens scanners (SOMATOM Definition Flash and Edge), only the noise was corrected by a factor of $1/(1.5)^{(1/2)}$[22,23].

Statistical analysis

Graphs for image noise *vs* radiation dose and SNR *vs* dose were evaluated for air, soft tissue and bone. Trend lines were determined for the data points using regression to produce power curves in MedCalc® Version 7.6.0.0 and

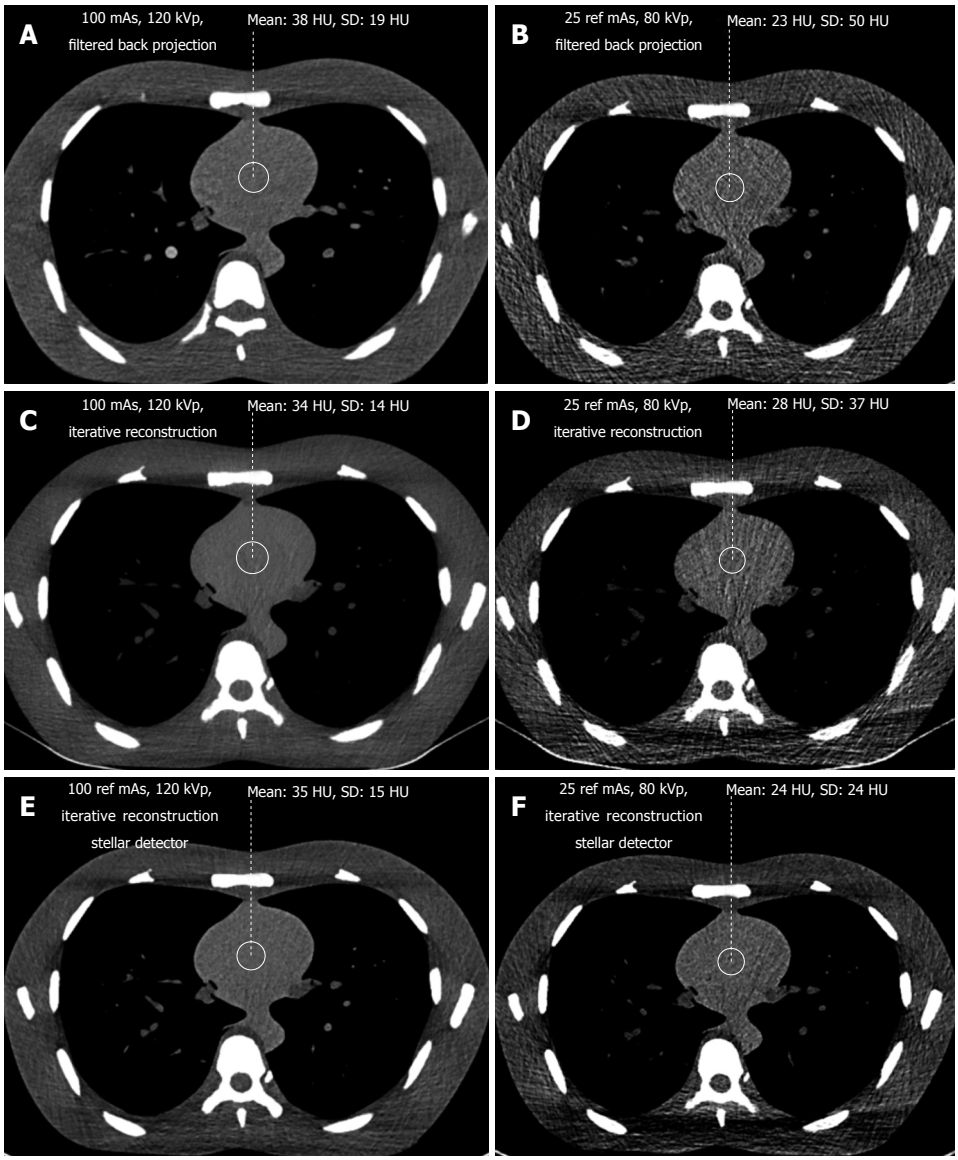

Figure 2 Soft tissue imaging using filtered back projection (A, B), iterative reconstruction (C, D, E, F) and the Stellar detector (E, F). At standard dose levels (A, C, E), image quality decreased from left to right. At the lowest dose level (B, D, F), the difference in noise increased. The image quality of the low dose image with the Stellar detector (F) was close to the image quality of that for a standard dose with a filtered back projection (A).

Microsoft Excel 2007. Noise reduction between two scanners was determined by subtracting the power curves. The integral of this subtraction equals the area between the curves. This area was divided by the dose to obtain the average noise reduction. The integral for the subtraction of the trend lines was calculated from the lowest (l) to the highest (h) joint radiation exposure according to

$$\int_l^h a \cdot x^b - c \cdot x^d \, dx = [(a \cdot x^{b+1})/(b+1) - (c \cdot x^{d+1})/(d+1)]$$

The dose reduction for a constant noise value was integrated along the noise scale to determine the average dose reduction. The smallest and highest reductions were determined to indicate the range. The Wilcoxon test for non-normally distributed paired samples was used to calculate the significance levels for noise reduction among the different scanners[30,31]. Inter-observer comparisons of the image quality score were performed, calculating the agreement levels with the Fleiss' K statistic[32,33]. The K strengths were categorized as follows: < 0.20 poor, 0.21-0.40 fair, 0.41-0.60 moderate, 0.61-0.80 good, and 0.81-1.00 very good[34]. The Wilcoxon test and the Fleiss' K statistic were analyzed in MedCalc® Version 7.6.0.0.

RESULTS

The noise levels measured in air, soft tissue and bone were significantly lower for iterative reconstruction compared to filtered back projection ($P < 0.0001$) and for using Stellar detectors in combination with IR compared to IR alone ($P < 0.0001$). The inter-observer agreement on image quality was moderate (kappa = 0.508). Noise/dose signature graphs for each scanner were plotted for air and soft tissue (Figures 3-5).

Soft tissue (mediastinum)

Noise reduction: The average noise reduction from fil-

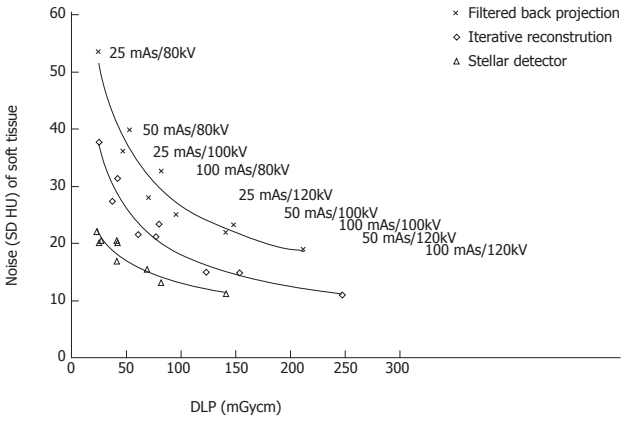

Figure 3 Noise for soft tissue imaging *vs* the radiation dose (dose-length product) for the different scanners. The improvement in the noise/dose was about the same for iterative reconstruction and the Stellar detector. The average noise reduction was approximately 30%. For the same image quality, the dose could be reduced by over 50%.

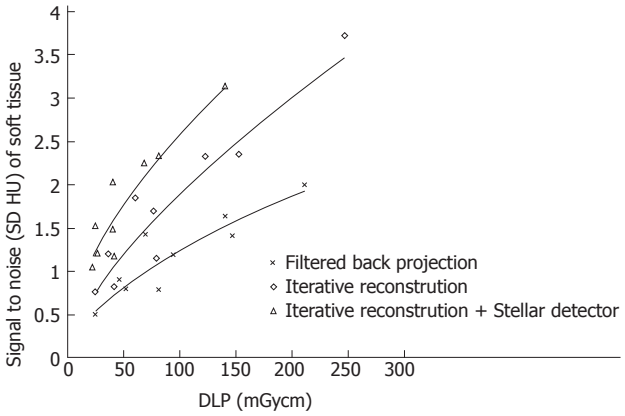

Figure 4 Signal to noise ratio *vs* radiation dose for the different scanners. Image quality was increased by 36% and 38% using iterative reconstruction and the Stellar detector, respectively.

tered back projection (FBP, SOMATOM Sensation) and iterative reconstruction (IR, Somatom Definition Flash) was 10 HU (7-15 HU) for the same radiation dose, generating 31% (30%-31%) less noise. Changing from IR to the Stellar detector (Sd, SOMATOM edge) allowed another 7 HU (4-16 HU) of noise to be removed. Noise was reduced on average by (32%); 24% for the highest dose and 42% for the lowest dose (Figure 3 and Table 1).

Dose reduction: For a constant noise level, the dose could be reduced by an average of 53 (25-116) mGycm by applying IR instead of FBP, corresponding to an average dose reduction of 52%. At the lowest dose (high noise level), the dose reduction was 50%. At the highest dose, the dose reduction was 55%. An additional 69 (46-96) mGycm reduction was possible using the Stellar detector (54%). More dose reduction was achieved for the highest noise level (65%) compared to the lowest noise level (39%, Table 1).

Signal to noise (SNR ranged from 0.5 to 3.7, Figure 4): When dose was held constant, the SNR could be increased on average to 0.7 (36%, ranging from 0.2 to 1) and 0.6 (38%, ranging from 0.5 to 0.8) using IR and IR/Stellar detectors, respectively. Using a constant SNR, the dose could be reduced on average by 59 mGycm (45%, ranging from 20 to 107 mGycm) and 52 mGycm (41%, ranging from 23 to 72 mGycm) for IR and IR/Sd, respectively (Figure 4 and Table 2).

Air

Noise reduction: A noise range of 23 to 118 HU was measured for all scans. Noise levels for Sd were always lower than for FBP, even when comparing the lowest dose of Sd against the highest dose of FBP (Figure 5). Noise at the same dose level could be lowered by 31 HU (44%) and 12 HU (31%) on average by changing from FBP to IR and from IR to Sd, respectively. The largest noise reductions were possible at lower dose levels (Figure 5, Table 1).

Dose reduction: To maintain a constant noise level, the dose was reduced by 133 (106-165) mGycm and 106 (65-166) mGycm when using IR instead of FBP and Sd instead of IR only, averaging dose reductions of 80% and 70%, respectively. The relative dose reductions were higher at higher noise levels (Figure 5, Table 1).

Bone: The noise ranged from 80 to 382 HU. The average noise reductions at constant radiation levels were 64 HU (30%) and 24 HU (15%) using IR and Sd, respectively. At higher dose levels, there was less noise reduction (Table 1). For a constant noise level, the doses could be lowered by 48 mGycm (30%) and 35 mGycm (27%) on average for IR and Sd, respectively. The dose reduction was higher at higher noise levels (Table 1).

Contrast to noise: With the same radiation dose, an average of 34% (22%-37%) and 25% (13%-46%) greater CNR was achieved by changing from FBP to IR and from IR to Sd, respectively. For the same CNR, the dose could be reduced on average by 59% (46%-71%) and 51% (38%-68%) for IR and Sd, respectively.

Subjective image quality (5 points maximal, Table 2): Image quality rose by 0.2 (0.1-0.4) points and 0.5 (0.2-0.9) points on average by changing from FBP to IR and from IR to Sd, respectively (Figure 6). For the same image quality, dose could be reduced by 25% (2%-42%) and 44% (33%-54%) using IR and Sd, respectively (Table 2).

DISCUSSION

By setting the image quality along with the noise, SNR and CNR, our study showed that iterative reconstruction and Stellar detectors produce better quality images than scans reconstructed with filtered back projection using lower CT doses. Using the SOMATOM Definition Flash instead of the Sensation enabled either a dose

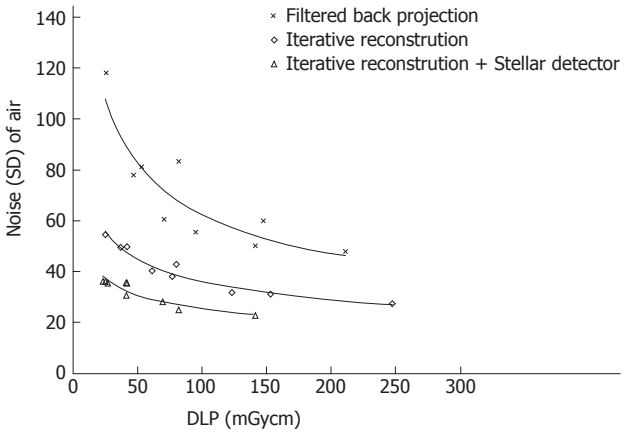

Figure 5 Image noise *vs* radiation dose in air. For pulmonary imaging, the noise reduction was 45% and 31% for iterative reconstruction and filtered back projection, respectively. For the Stellar detector and iterative reconstruction alone, the average dose reduction was 80% and 70%, respectively.

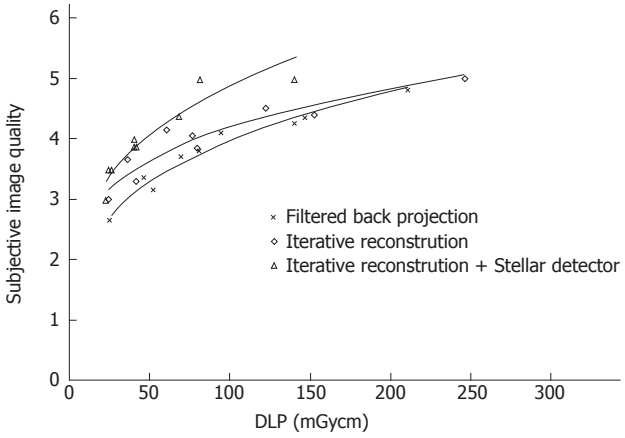

Figure 6 Subjective image quality *vs* dose. Subjective image quality increased on average from 0.2 to 0.5 using iterative reconstruction and the Stellar detector on a scale from 1 to 5, 5 being the maximum.

reduction of 80% or a noise reduction of 44% when imaging air. It is not possible to achieve simultaneous dose and noise reduction. Additionally, at the level of maximal dose reduction, it is not possible to further increase image quality and vice versa. It is known that iterative reconstruction approaches (Adaptive Statistical Iterative Reconstruction or Sinogram Affirmed Iterative Reconstruction) can in some cases reduce radiation dose by 27% to 65%[13-18]. Our phantom study results confirm these findings, showing dose reductions of 30%, 52% and 80% for imaging bone, soft tissue and air, respectively.

Using the recently introduced Stellar detector, signal-transformation was implemented into the detector itself to reduce electronic noise. With this technique, it was possible to further reduce radiation dose by an average 27%, 54% and 70% for bone, soft tissue and air, respectively.

With lower tube voltage, not only did the image noise increase, but the density of the bone also increased, which is well known for dual energy scans. When the signal increased, the SNR also increased, altering the bone diagram. This is most likely the main reason why the Stellar detectors did not have the same effect on dose reduction when imaging bone. The benefit of dose reduction is greater for low doses, especially for bone and air. The absolute dose reduction, measured in mGy-cm, was larger at high doses, but the relative reduction was always larger at lower doses. This was true with the exceptions of subjective image quality and SNR, which are influenced by increased signal at lower doses (such as the case of bone). The manufacturer claims that Stellar detectors reduce noise by 20%[19]. However, because dose increases by a power of 2 as noise decreases, a potential dose reduction of 36% should be possible. We produced dose reductions of 27%-70% and noise reductions of 15%-32%. As mentioned above, the lower the dose levels, the bigger the relative benefit. Our scan range covered only low dose levels, with a high dose of 250 mGycm (100 reference mAs/120 kVp), equivalent to approximately 3 mSv. At high dose levels, the noise reduction approached 20% (24%, 28% and 7% for air, soft tissue and bone, respectively). The noise level was strongly influenced by the chosen kernel. For FBP reconstruction, there was a tradeoff between spatial resolution and noise. This tradeoff could be adjusted by selecting different kernels. Soft tissue kernels had much lower standard deviations in the signal than hard kernels for air and bone. Therefore, it was necessary to use the same kernels for comparisons. Some radiation protectors believe that the risk from high radiation (atomic bombs) can be extrapolated to much lower radiation exposures (CT) and that the risk of death due to radiation-induced cancer for the general population is 0.005%/mSv[35]. The conversion coefficient from DLP to mSv is 0.014 for lung[36,37], equivalent to a reduction of radiation induced cancer death per chest CT from 1 in 13000 for iterative reconstruction to 1 in 32000 when using Stellar detectors. These estimates neglect the potential bio-positive effects of low radiation exposure[38-42]. Nevertheless, radiation is a cumulative physical quantity that may lead to stochastic processes such as carcinogenesis. Therefore, radiation protection is mandatory even at lower dose levels.

In a previous phantom study using the SOMATOM Sensation, it was shown that the sensitivity for lung nodule detection was not significantly altered for images acquired with 50 mAs and 80 kVp compared to 100 mAs and 120 kVp (article submitted). With the findings from our present study, it is possible to transfer these parameters to new scanners that use iterative reconstruction and better detectors. Our images had noise levels of 81 and 40 HU for air and mediastinum, respectively. For similar noise levels, parameters as low as 25 mAs and 80 kVp for the SOMATOM Definition Flash and Edge are theoretically sufficient for detection without loss of sensitivity (Figures 3-5).

Obviously, image quality is not only defined by signal

Table 1 Reduction of noise and dose using iterative reconstruction and the stellar detector

	Soft tissue				Air				Bone			
		Lowest dose		Highest dose		Lowest dose		Highest dose		Lowest dose		Highest dose
	Δ HUsd	Range			Δ HUsd	Range			Δ HUsd	Range		
Noise reduction from FBP to IR	10 (31%)	15 (30%)	to	7 (31%)	31 (44%)	53 (49%)	to	22 (41%)	64 (30%)	128 (37%)	to	28 (21%)
Noise reduction from IR to IR with Sd	7 (32%)	16 (42%)	to	4 (24%)	12 (31%)	19 (34%)	to	9 (28%)	24 (15%)	51 (22%)	to	9 (7%)
	Δ DLP	Range			Δ DLP	Range			Δ DLP	Range		
Dose reduction from FBP to IR for the same noise level	53 (52%)	116 (55%)	to	25 (50%)	133 (80%)	165 (78%)	to	106 (81%)	48 (30%)	24 (12%)	to	40 (55%)
Dose reduction from IR to IR with Sd for the same noise level	69 (54%)	96 (39%)	to	46 (65%)	106 (70%)	166 (67%)	to	65 (72%)	35 (27%)	33 (21%)	to	25 (43%)

HUsd: Noise (sd of Hounsfield Units); FBP: Filtered back projection; IR: Iterative reconstruction; Sd: Stellar detector; DLP: Dose length product.

Table 2 Dose, signal to noise ratio and improved subjective image quality using iterative reconstruction and the stellar detector

	Soft tissue					lung			
	Δ HUsd	Range				Δ Points	Range		
		Lowest dose		Highest dose			Lowest dose		Highest dose
Signal to noise reduction from FBP to IR	0.7 (36%)	0.2 (31%)	to	1 (39%)	Improving subjective image quality from FBP to IR	0.2 (7%)	0.4 (13%)	to	0.1 (3%)
Signal to noise reduction from IR to IR with Sd	0.6 (38%)	0.5 (41%)	to	0.8 (32%)	Improving subjective image quality from IR to IR with Sd	0.5 (13%)	0.2 (8%)	to	0.9 (17%)
	Δ DLP	Range				Δ DLP	Range		
		Lowest SNR		Highest SNR			lowest SNR		highest SNR
Dose reduction from FBP to IR for the same SNR	59 (45%)	20 (40%)	to	107 (47%)	Dose reduction from FBP to IR for same subjective quality	19 (25%)	22 (42%)	to	5 (2%)
Dose reduction from IR to IR with Sd for the same SNR	52 (41%)	23 (49%)	to	72 (36%)	Dose reduction from IR to IR with Sd for same subjective quality	57 (44%)	10 (33%)	to	130 (54%)

HUsd: Noise (sd of Hounsfield Units); FBP: Filtered back projection; IR: Iterative reconstruction; Sd: Stellar detector; DLP: Dose length product; SNR: Signal to noise ratio.

but also by contrast and noise because a loss of subjective image quality is less impressive than an increase in noise level. In other words, radiologists rate image quality higher than the measured noise would suggest. Perception of image quality is influenced by spatial resolution, individual vision and pattern recognition, all of which cannot be precisely measured. Fortunately, subjective image quality was not rated below what the noise level would predict.

Limitations

Noise is one parameter of image quality, but we did not investigate scan plane and z-axis spatial resolution (Z-sensitivity) or high-contrast resolution[22]. Further studies are needed to investigate these parameters to understand how the type of scanner can influence image quality. The pre-settings for THORAX ROUTINE were not the same for the three scanner types. For example, the pitch for the Sensation was 0.8, but this value was altered to 0.6 for the other scanners. Increasing the pitch from 0.6 to 0.8 did not change the noise; however, the dose decreased corresponding to a Siemens specific unchanged tube current time product/pitch[43]. Therefore, it is possible that the images acquired by the Somatom Sensation have slightly different dose levels at lower pitches. The resolution was slightly different for the B- and I-Kernels for the different reconstruction approaches, which might have negatively influenced the noise of the I-Kernel. Ongoing studies will address this topic.

As varying kVp lead to CT number changes, it can be difficult to interpret results, especially for SNR and CNR. Possible differences in gantry geometry, detector efficiency and tube spectrum for the three investigated scanners were also neglected because our intent was to give an approximation of dose and noise reduction among the last three generations of CT for given clinical presettings. Varying the kVp also provoked questions about how beam-hardening effects impact the images, which will require further investigation.

To evaluate the dose reduction provided by the new Stellar detector, it would be desirable to compare images reconstructed using the FBP algorithm, which is a linear algorithm with predictable performance. We only compared SAFIRE reconstructed images with and without the Stellar detector. Due to the nonlinearity of iterative reconstruction methods, reconstruction may be object and dose dependent. Thus, it is difficult to characterize the improvements provided by the Stellar detector alone from the results in our study. Further investigations need to address this topic.

In conclusion, this study demonstrated an average dose reduction of 27% to 70% by applying the new Stellar detector. This dose reduction was equivalent to using IR instead of FBP.

COMMENTS

Background

Due to increasing computing capacity, iterative image reconstruction can be introduced into clinics, leading to the potential for dose reduction by replacing older filtered back projection methods. The problem of electronic noise during image acquisition was overcome by integrating the analog-digital-converter with the photodiode of the computed tomography (CT)-detectors on the same silicon chip. This noise reduction can either be used for dose reduction or to increase the image quality. The three latest CT-scanner generations were examined to compare their potential for dose reduction.

Research frontiers

Several studies demonstrated the feasibility of low dose imaging without loss of sensitivity for pulmonary diseases. Radiologists are able to lower the CT tube current and/or the tube voltage, using the lowest acceptable published dose levels for older CT scanners. Manufacturer dependent progress in CT-technology was only partly investigated. Dose or noise reduction using iterative reconstruction has been published, but the potential for new detectors in the clinic is not yet known.

Innovations and breakthroughs

This study demonstrates the dependency of CT radiation dose, image quality and CT-generation. It is possible to obtain the same image quality with a dose reduction of 30% to 80% by substituting filtered back projection with iterative image reconstruction. Using the new CT-detectors, radiation dose can be reduced by an additional 27% to 70%, depending on the scanned tissue.

Applications

With the results, the lowest acceptable tube currents and voltages for the older CT-generations can be transferred to the newest scanners.

Terminology

CT-exams produce cross sectional images of the body, based on the radiation absorption of the body tissues. Radiation absorption is measured at every angle circularly around the body and is back-projected on a virtual pixel field in the scanned plane, delivering a filtered back projection image. New iterative reconstruction methods distribute the absorption of one angle to all of the pixels in a direction, adjusting the pixel values based on the effective absorption for each angle position. For clinical routines, three iterations of 360° rotation are used, which is very time-consuming. Only recently was it possible to deliver sufficient computing power for these clinical scanners.

Peer review

This manuscript described an interest work that the average dose could be reduced 30%, 52% and 80% for imaging bone, soft tissue and air for the same image quality by using iterative reconstruction instead of filtered back projection. In addition, employing the new Stellar detector could further lower radiation dose additionally by 27%, 54% and 70% for bone, soft tissue and air, respectively. The manuscript can be accepted for publication as it is.

REFERENCES

1 **Kalender WA**, Wolf H, Suess C. Dose reduction in CT by anatomically adapted tube current modulation. Ⅱ. Phantom measurements. *Med Phys* 1999; **26**: 2248-2253 [PMID: 10587205 DOI: 10.1118/1.598738]

2 **Kalra MK**, Maher MM, Toth TL, Schmidt B, Westerman BL, Morgan HT, Saini S. Techniques and applications of automatic tube current modulation for CT. *Radiology* 2004; **233**: 649-657 [PMID: 15498896 DOI: 10.1148/radiol.2333031150]

3 **Graser A**, Wintersperger BJ, Suess C, Reiser MF, Becker CR. Dose reduction and image quality in MDCT colonography using tube current modulation. *AJR Am J Roentgenol* 2006; **187**: 695-701 [PMID: 16928932 DOI: 10.2214/AJR.05.0662]

4 **Greess H**, Wolf H, Baum U, Kalender WA, Bautz W. [Dosage reduction in computed tomography by anatomy-oriented attenuation-based tube-current modulation: the first clinical results]. *Rofo* 1999; **170**: 246-250 [PMID: 10230432 DOI: 10.1007/s003300050062]

5 **Mulkens TH**, Bellinck P, Baeyaert M, Ghysen D, Van Dijck X, Mussen E, Venstermans C, Termote JL. Use of an automatic exposure control mechanism for dose optimization in multi-detector row CT examinations: clinical evaluation. *Radiology* 2005; **237**: 213-223 [PMID: 16126917 DOI: 10.1148/radiol.2363041220]

6 **Gies M**, Kalender WA, Wolf H, Suess C. Dose reduction in CT by anatomically adapted tube current modulation. I. Simulation studies. *Med Phys* 1999; **26**: 2235-2247 [PMID: 10587204 DOI: 10.1118/1.598779]

7 **Kojima H**, Tsujimura A, Yabe H. [Usefulness of the adaptive dose shield for the infant CT]. *Nihon Hoshasen Gijutsu Gakkai Zasshi* 2011; **67**: 57-61 [PMID: 21301172 DOI: 10.6009/jjrt.67.57]

8 **Hein E**, Rogalla P, Klingebiel R, Hamm B. Low-dose CT of the paranasal sinuses with eye lens protection: effect on image quality and radiation dose. *Eur Radiol* 2002; **12**: 1693-1696 [PMID: 12111059 DOI: 10.1007/s00330-001-1279-9]

9 **Hopper KD**, King SH, Lobell ME, TenHave TR, Weaver JS. The breast: in-plane x-ray protection during diagnostic thoracic CT--shielding with bismuth radioprotective garments. *Radiology* 1997; **205**: 853-858 [PMID: 9393547]

10 **Hopper KD**. Orbital, thyroid, and breast superficial radiation shielding for patients undergoing diagnostic CT. *Semin Ultrasound CT MR* 2002; **23**: 423-427 [PMID: 12509112 DOI: 10.1016/S0887-2171(02)90013-2]

11 **Hopper KD**, Neuman JD, King SH, Kunselman AR. Radioprotection to the eye during CT scanning. *AJNR Am J Neuroradiol* 2001; **22**: 1194-1198 [PMID: 11415918]

12 **McLaughlin DJ**, Mooney RB. Dose reduction to radiosensitive tissues in CT. Do commercially available shields meet the users' needs? *Clin Radiol* 2004; **59**: 446-450 [PMID: 15081850 DOI: 10.1016/j.crad.2003.10.016]

13 **Pontana F**, Duhamel A, Pagniez J, Flohr T, Faivre JB, Hachulla AL, Remy J, Remy-Jardin M. Chest computed tomography using iterative reconstruction vs filtered back projection (Part 2): image quality of low-dose CT examinations in 80 patients. *Eur Radiol* 2011; **21**: 636-643 [PMID: 21080171 DOI: 10.1007/s00330-010-1991-4]

14 **Leipsic J**, Labounty TM, Heilbron B, Min JK, Mancini GB, Lin FY, Taylor C, Dunning A, Earls JP. Estimated radiation dose reduction using adaptive statistical iterative reconstruction in coronary CT angiography: the ERASIR study. *AJR Am J Roentgenol* 2010; **195**: 655-660 [PMID: 20729443 DOI: 10.2214/AJR.10.4288]

15 **Singh S**, Kalra MK, Shenoy-Bhangle AS, Saini A, Gervais DA, Westra SJ, Thrall JH. Radiation dose reduction with hybrid iterative reconstruction for pediatric CT. *Radiology* 2012; **263**: 537-546 [PMID: 22517962 DOI: 10.1148/radiol.12110268]

16 **Hara AK**, Paden RG, Silva AC, Kujak JL, Lawder HJ, Pavlicek W. Iterative reconstruction technique for reducing body radiation dose at CT: feasibility study. *AJR Am J Roentgenol* 2009; **193**: 764-771 [PMID: 19696291 DOI: 10.2214/AJR.09.2397]

17 **Kalra MK**, Woisetschläger M, Dahlström N, Singh S, Lindblom M, Choy G, Quick P, Schmidt B, Sedlmair M, Blake MA, Persson A. Radiation dose reduction with Sinogram Affirmed Iterative Reconstruction technique for abdominal computed tomography. *J Comput Assist Tomogr* 2012; **36**: 339-346 [PMID: 22592621 DOI: 10.1097/RCT.0b013e31825586c0]

18 **Winklehner A**, Karlo C, Puippe G, Schmidt B, Flohr T, Goetti R, Pfammatter T, Frauenfelder T, Alkadhi H. Raw data-based iterative reconstruction in body CTA: evaluation of radiation dose saving potential. *Eur Radiol* 2011; **21**: 2521-2526 [PMID: 21822785 DOI: 10.1007/s00330-011-2227-y]

19 **Ulzheimer S**. Stellar Detector Performance in Computed

Tomography: The first fully-integrated detector in the CT industry sets a new reference in image quality with HiDynamics, TrueSignal and Ultra Fast Ceramics. *Somatom Sessions* 2011; **29**: 64-66
20 **Romans L**. Introduction to Computed Tomography. Baltimore, MD: Williams & Wilkins, 1995
21 **Seeram E**. Computed Tomography: Physical Principles, Clinical Applications & Quality Control. Philadelphia, Penn: WB Saunders Co., 1994
22 **Goldman LW**. Principles of CT: radiation dose and image quality. *J Nucl Med Technol* 2007; **35**: 213-225; quiz 226-228 [PMID: 18006597 DOI: 10.2967/jnmt.106.037846]
23 **Stoyanov D**, Vassileva J. Influence of exposure parameters on patient dose and image noise in computed tomography. *Pol J Med Phys Eng* 2009; **15**: 215-226
24 **Shuman WP**, Branch KR, May JM, Mitsumori LM, Lockhart DW, Dubinsky TJ, Warren BH, Caldwell JH. Prospective versus retrospective ECG gating for 64-detector CT of the coronary arteries: comparison of image quality and patient radiation dose. *Radiology* 2008; **248**: 431-437 [PMID: 18552312 DOI: 10.1148/radiol.2482072192]
25 **Diederich S**, Lenzen H, Windmann R, Puskas Z, Yelbuz TM, Henneken S, Klaiber T, Eameri M, Roos N, Peters PE. Pulmonary nodules: experimental and clinical studies at low-dose CT. *Radiology* 1999; **213**: 289-298 [PMID: 10540674]
26 **Christe A**, Lin MC, Yen AC, Hallett RL, Roychoudhury K, Schmitzberger F, Fleischmann D, Leung AN, Rubin GD, Vock P, Roos JE. CT patterns of fungal pulmonary infections of the lung: comparison of standard-dose and simulated low-dose CT. *Eur J Radiol* 2012; **81**: 2860-2866 [PMID: 21835569 DOI: 10.1016/j.ejrad.2011.06.059]
27 **Weng MJ**, Wu MT, Pan HB, Kan YY, Yang CF. The feasibility of low-dose CT for pulmonary metastasis in patients with primary gynecologic malignancy. *Clin Imaging* 2004; **28**: 408-414 [PMID: 15531140 DOI: 10.1016/S0899-7071(03)00246-8]
28 **Gergely I**, Neumann C, Reiger F, Dorffner R. [Lung nodule detection with ultra-low-dose CT in routine follow-up of cancer patients]. *Rofo* 2005; **177**: 1077-1083 [PMID: 16021539 DOI: 10.1055/s-2005-858370]
29 **Schindera ST**, Graca P, Patak MA, Abderhalden S, von Allmen G, Vock P, Szucs-Farkas Z. Thoracoabdominal-aortoiliac multidetector-row CT angiography at 80 and 100 kVp: assessment of image quality and radiation dose. *Invest Radiol* 2009; **44**: 650-655 [PMID: 19724236 DOI: 10.1097/RLI.0b013e3181acaf8a]
30 **Zwillinger D**. Standard mathematical Tables and Formula. A Chapman & Hall Book. Boca Raton, Florida: CRC Press LLC, 2003: e. 31st e
31 **Altman DG**. Practical statistics for medical research. London: Chapman and Hall, 1991
32 **Fleiss JL**. Measuring nominal scale agreement among many raters. *Psychol Bull* 1971; **76**: 378-383 [DOI: 10.1037/h0031619]
33 **Fleiss JL**. Statistical methods for rates and proportions. 2nd edition. New York: John Wiley, 1981; 38-46
34 **Landis JR**, Koch GG. The measurement of observer agreement for categorical data. *Biometrics* 1977; **33**: 159-174 [PMID: 843571 DOI: 10.2307/2529310]
35 **National Council on Radiation Protection and Measurements.** Risk estimations for radiation protection. NCRP report No. 115, Bethesda, Maryland, December 31, 1993. ISBN 0-929600-34-7
36 **Shrimpton P**. Assessment of patient dose in CT: Appendix C. In: European guidelines for multislice computed tomography funded by the European Commission 2004: contract number FIGMCT2000-20078-CT-TIP. Luxembourg: European Commission, 2004
37 **Shrimpton PC**, Hillier MC, Lewis MA, Dunn M. Doses from computed tomography (CT) examinations in the UK: 2003 review. Chilton, UK: National Radiological Protection Board, 2005: report NRPB-W67
38 **Yang J**, Yu Y, Hamrick HE, Duerksen-Hughes PJ. ATM, ATR and DNA-PK: initiators of the cellular genotoxic stress responses. *Carcinogenesis* 2003; **24**: 1571-1580 [PMID: 12919958 DOI: 10.1093/carcin/bgg137]
39 **Ye N**, Bianchi MS, Bianchi NO, Holmquist GP. **Adaptive** enhancement and kinetics of nucleotide excision repair in humans. *Mutat Res* 1999; **435**: 43-61 [PMID: 10526216 DOI: 10.1016/S0921-8777(99)00022-1]
40 **Yu Y**, Okayasu R, Weil MM, Silver A, McCarthy M, Zabriskie R, Long S, Cox R, Ullrich RL. Elevated breast cancer risk in irradiated BALB/c mice associates with unique functional polymorphism of the Prkdc (DNA-dependent protein kinase catalytic subunit) gene. *Cancer Res* 2001; **61**: 1820-1824 [PMID: 11280730]
41 **Yukawa O**, Nakajima T, Yukawa M, Ozawa T, Yamada T. Induction of radical scavenging ability and protection against radiation-induced damage to microsomal membranes following low-dose irradiation. *Int J Radiat Biol* 1999; **75**: 1189-1199 [PMID: 10528927 DOI: 10.1080/095530099139665]
42 **Zeeb H**, Blettner M, Langner I, Hammer GP, Ballard TJ, Santaquilani M, Gundestrup M, Storm H, Haldorsen T, Tveten U, Hammar N, Linnersjö A, Velonakis E, Tzonou A, Auvinen A, Pukkala E, Rafnsson V, Hrafnkelsson J. Mortality from cancer and other causes among airline cabin attendants in Europe: a collaborative cohort study in eight countries. *Am J Epidemiol* 2003; **158**: 35-46 [PMID: 12835285 DOI: 10.1093/aje/kwg107]
43 **Flohr TG**, Leng S, Yu L, Aiimendinger T, Bruder H, Petersilka M, Eusemann CD, Stierstorfer K, Schmidt B, McCollough CH. Dual-source spiral CT with pitch up to 3.2 and 75 ms temporal resolution: image reconstruction and assessment of image quality. *Med Phys* 2009; **36**: 5641-5653 [PMID: 20095277 DOI: 10.1118/1.3259739]

P- Reviewer: Meng LJ **S- Editor**: Wen LL
L- Editor: A **E- Editor:** Liu XM

百世登

Baishideng®

Published by **Baishideng Publishing Group Co., Limited**
Flat C, 23/F., Lucky Plaza,
315-321 Lockhart Road, Wan Chai,
Hong Kong, China
Fax: +852-65557188
Telephone: +852-31779906
E-mail: bpgoffice@wjgnet.com
http://www.wjgnet.com